ANALYSIS OF SMITH-PURCELL BWO WITH END REFLECTIONS *

Vinit Kumar†,RRCAT, Indore, M.P. 452013,INDIA
Kwang-Je Kim, ANL, Argonne, IL 60439,USA.

Abstract

We present a one-dimensional time-dependent analysis and simulation of Smith-Purcell (SP) backward wave oscillator (BWO) taking end reflections and attenuation into account. In the linear regime, we obtain an analytic solution and calculate the start current. The dependence of start current on end reflections is studied taking the attenuation due to finite conductivity into account.

INTRODUCTION

The Smith-Purcell (SP) free-electron laser in the terahertz (THz) regime using a low energy electron beam is a backward wave oscillator (BWO) [1,2]. Previous analyses of SP-BWO [1-3] have ignored the reflection at the ends of the grating. However, there will in general be some reflection at the end of the grating due to discontinuity in the medium. One can, if desired, also add external mirrors to enhance reflection. In the presence of reflection, the start current, which is defined as the minimum value of the electron beam current needed to produce coherent electromagnetic oscillations, can be reduced. In this paper, we present a self consistent nonlinear analysis of SP-BWO including end reflections and attenuation. We set up Maxwell-Lorentz equations equations and develop a computer code to solve these equations. We present the results of numerical simulation and discuss the evolution of power. In the linear regime, we solve the coupled Maxwell-Lorentz equations analytically and calculate the start current taking end reflection and attenuation into account.

MAXWELL-LORENTZ EQUATIONS

In a SP-BWO, the electron beam interacts with the backward surface wave co-propagating with the electron beam. We assume that the electron beam is in the form of a thin sheet moving along the z-axis above a metal grating with rectangular grooves, the direction of the grooves is along the y-axis and the outward normal to the grating surface is along the x-axis. The plane of the sheet electron beam is at x = 0, and the top surface of the grating is at $x = -b$. We have earlier studied the interaction between the electron beam and the backward surface mode using Maxwell-Lorentz equations where we ignored the reflection at the end of the grating [2]. The backward surface mode supported by the grating is a linear combination of infinite number of Floquet-Bloch harmonics having the z-component of propagation vectors differing from each other by an integral multiple of k_g, where $k_g = 2\pi/\lambda_g$ and λ_g is the period of the grating. The y-component H_y of the magnetic field of the backward surface mode can be written as $\sum A_n \exp(ik_0 z + ink_g z - \Gamma_n x - i\omega t)$, where the summation is implied over all n from -∞ to +∞ [2]. Here, ω is the frequency, k_0 is the propagation vector of the backward surface mode, $\Gamma_n = \sqrt{(k_0 + nk_g)^2 - \omega^2/c^2}$ and c is the speed of light. The zeroth-order component of this mode has the longitudinal electric field given by $E_-(z,t)\exp(ik_0 z - i\omega t)$ at $x = 0$. The amplitude of all other components of the backward surface mode have to maintain a fixed ratio with the amplitude of the zeroth-order component such that the electromagnetic field satisfies the required boundary conditions. Hence, as the zeroth-order component of the surface mode evolves due to interaction with co-propagating electron beam, the amplitude of all other components also evolve proportionately. One can calculate the group velocity, which is $d\omega/dk$, from the dispersion relation of the backward surface mode. For low energy electron beam, the group velocity of the co-propagating surface mode having $\omega/k_0 = \beta c$ is along the negative z-axis [1,2]. Let us denoted the magnitude of the group velocity by v_g. Here, βc is the velocity of electrons.

For a grating with rectangular grooves considered here, a wave going along the positive z-axis will see the same boundary as the wave going along the negative z-axis. Hence, if we construct a mode having H_y given by $\sum A_n \exp(-ik_0 z - ink_g z - \Gamma_n x - i\omega t)$, it will satisfy the Maxwell equations and the required boundary condition for the reflection grating. This is actually the forward surface mode supported by the grating. This has the propagation vector -k_0 and the group velocity v_g along the positive z-axis. Hence, the grating supports forward as well as backward surface mode. However, none of the components of the forward surface mode co-propagate with the electron beam. Consequently, the forward surface mode does not interact with the electron beam. It however arises due to reflection of the backward wave at the end of the grating. As the backward surface mode extracts energy from the electron beam and grows, it gets reflected at the end to the forward surface mode and consequently the forward surface mode also grows. Let us denote the zeroth-order component of the forward surface mode as $E_+(z,t)\exp(-ik_0 z - i\omega t)$ at the location of sheet electron beam.

In our previous work [2], we had set up Maxwell equation for the backward wave, which is coupled to Lorentz equations for the beam dynamics. We will now add the Maxwell equation for the forward wave to this set of equa-

* Work supported by U.S. Department of Energy, Office of Basic Energy Sciences, under Contract No. W-31-109-ENG-38.
† vinit@cat.ernet.in

tions. We will be following notations used in Ref. 2. The energy flows along the negative z-axis for the backward wave and hence, it gets attenuated along the negative z-axis. Similarly, for the forward wave, the energy flows along the positive z-axis and it gets attenuated along the positive z-axis. The complex attenuation coefficient α for the backward wave supported by a rectangular reflection grating can be obtained as per the prescription given in Ref. 3. For the forward wave, the complex attenuation coefficient will be simply $-\alpha$. Taking the attenuation into account, the equation for the evolution of the amplitude E_+ of the forward wave becomes

$$\frac{\partial E_+}{\partial z} + \frac{1}{v_g}\frac{\partial E_+}{\partial t} = -\alpha E_+. \quad (1)$$

The equation for the evolution of the amplitude E_- of the backward wave as derived earlier is given by [2,4]

$$\frac{\partial E_-}{\partial z} - \frac{1}{v_g}\frac{\partial E_-}{\partial t} = \frac{IZ_0\chi}{2\beta\gamma\Delta y} e^{-2\Gamma_0 b}\langle e^{-i\psi}\rangle + \alpha E_-, \quad (2)$$

where I is the electron beam current, Z_0 = 377 Ω is the characteristic impedence of free space, χ is the residue of the singularity associated with the surface mode as defined in Ref. 2, γ is the energy of the electron beam in unit of rest energy, ψ is the electron phase and Δy is the width of the sheet electron beam in the y-direction. Both these equations are coupled through boundary condition at the end of the grating. Let ρ_0 and ρ_L be the complex reflection coefficient at the entrance and exit end of the grating. The boundary conditions will then given by $E_+(z = 0) = \rho_0 E_-(z = 0)$, and $E_-(z = L)e^{ik_0 L} = \rho_L E_+(z = L)e^{-ik_0 L}$, where L is the length of the grating. The entrance and the exit of the grating are at z = 0 and $z = L$ respectively.

In order to further simplify the analysis, we define a new amplitude of the forward wave given by $E_+ = -\rho_0\tilde{E}_+$. The boundary conditions, in term of this definition can then be written as $\tilde{E}_+(z = 0) = -E(z = 0)$ and $E_-(z = L) = \mathcal{R}e^{-i2k_0 L}\tilde{E}_+(Z = L)$, where $\mathcal{R} = -\rho_0\rho_L$. As discussed in Ref. 2, we can define dimensionless variables and make a transformation from (z, t) to (ζ, τ) to simplify the analysis. Here, $\zeta = z/L$ is the normalised length and τ is the dimensionless time defined in Ref. 2. We define dimensionless amplitude of the forward and the backward wave denoted by $\mathcal{E}_+$ and $\mathcal{E}_-$ respectively as

$$\mathcal{E}_\pm = \frac{4\pi}{I_A Z_0}\frac{k_0 L^2}{\beta^2\gamma^3}\tilde{E}_\pm\ , \quad (3)$$

where I_A = 17 kA is the Alfvén current and $\tilde{E}_- = E_-$. After making these transformations, the equation for evolution of $\mathcal{E}_+$ and $\mathcal{E}_-$ are given by

$$\frac{\partial \mathcal{E}_-}{\partial \tau} - \frac{\partial \mathcal{E}_-}{\partial \zeta} = -\mathcal{J}\langle e^{-i\psi}\rangle - \alpha L\mathcal{E}_-, \quad (4)$$

$$\frac{\partial \mathcal{E}_+}{\partial \tau} + d_1\frac{\partial \mathcal{E}_+}{\partial \zeta} = -d_1\alpha L\mathcal{E}_+, \quad (5)$$

where $d_1 = (v_p + v_g)/(v_p - v_g)$. The boundary conditions now become $\mathcal{E}_+(\zeta = 0) = -\mathcal{E}_-(\zeta = 0)$ and $\mathcal{E}_-(\zeta = 1) = \mathcal{R}e^{-i2k_0 L}\mathcal{E}_+(\zeta = 1)$. These equations are coupled to the electron beam dynamics equations

$$\frac{\partial \eta_i}{\partial \zeta} = (\mathcal{E}_- + \mathcal{E}_{sc})e^{i\psi_i} + c.c., \quad (6)$$

$$\frac{\partial \psi_i}{\partial \zeta} = \eta_i, \quad (7)$$

where the $\mathcal{E}_{sc}$ is the dimensionless longitudinal electric field due to space charge given by $\mathcal{E}_{sc} = iQ\langle e^{-i\psi}\rangle$, and $Q = (\mathcal{J}/\chi L)(\chi_1 - e^{2\Gamma_0 b})$. The χ_1-parameter appears in the analysis of singularity associated with the surface mode and can be calculated as per prescription discussed in Ref. 2. Here the subscript i stands for i^{th} electron and $\eta_i = (\gamma_i - \gamma)/\gamma$ is the relative energy deviation of the i^{th} electron. Eqs. (4-7) along with the boundary conditions form the complete set of differential equations needed to describe the one-dimensional time-dependent behavior of SP-BWO with end reflections and attenuation. In the next section, we discuss the analytic solution of these equations in the linear regime.

LINEAR ANALYSIS

We can linearize Eqs. (4-7) around an equilibrium solution and perform a stability analysis to find out the parameter regime in which the instability for exchange of energy from electron beam to electromagnetic oscillation can be excited. For simplicity, let us assume that the injected beam is monoenergetic, and η_i = 0 for all the electrons at ζ = 0. Further, we assume that the injected beam is unbunched, i.e., $\langle e^{-i\psi_0}\rangle$ = 0, where $\psi_{0,i}$ is the phase of the i^{th} particle at ζ = 0. An equilibrium solution of the system of Eqs. (4-7) is obviously $\mathcal{E}_- = 0, \mathcal{E}_+ = 0, \eta_i = 0$, and $\psi_i = \psi_{0,i}$. Let us define the perturbative solution by $\mathcal{E}_- = \tilde{\epsilon}_-$, $\mathcal{E}_+ = \tilde{\epsilon}_+$, $\eta_i = \delta\eta_i$, and $\psi_i = \psi_{0,i} + \delta\psi_i$. We introduce the following collective variables as done by Bonifacio et al. [5] for conventional FELs:

$$\tilde{x} = \langle \delta\psi e^{-i\psi_0}\rangle, \qquad \tilde{y} = \langle \delta\eta e^{-i\psi_0}\rangle. \quad (8)$$

In terms of these variables, Eqs. (4-7) can be linearized and written as

$$\frac{\partial \tilde{\epsilon}_-}{\partial \tau} - \frac{\partial \tilde{\epsilon}_-}{\partial \zeta} = i\mathcal{J}\tilde{x} - \alpha L\tilde{\epsilon}_-, \quad (9)$$

$$\frac{\partial \tilde{\epsilon}_+}{\partial \tau} + d_1\frac{\partial \tilde{\epsilon}_+}{\partial \zeta} = -d_1\alpha L\tilde{\epsilon}_+, \quad (10)$$

$$\frac{\partial \tilde{x}}{\partial \zeta} = \tilde{y}, \quad (11)$$

$$\frac{\partial \tilde{y}}{\partial \zeta} = \tilde{\epsilon}_- + Q\tilde{x}. \quad (12)$$

The boundary conditions for these equations are: (1) $\tilde{x} = 0$ at ζ = 0 at all τ since the injected beam has no phase modulation, i.e., it is injected unbunched. (2) $\tilde{y} = 0$ at ζ =

0 at all τ since the injected beam has no energy modulation, i.e., it is injected monoenergetically. (3) $\tilde{\epsilon}_+ = -\tilde{\epsilon}_-$ at $\zeta = 0$ for all τ, and $\tilde{\epsilon}_- = \mathcal{R}e^{-i2k_0L}\tilde{\epsilon}_+$ at $\zeta = 1$ for all τ. Assuming a solution of the type $e^{\nu\tau}$, we can find out the growth rate ν for the above linearised equations with the boundary conditions. In order to find out the growth rate ν, one has to first solve the following cubic equation

$$\kappa^3 - (\nu + \alpha L)\kappa^2 - Q\kappa + \nu Q + i\mathcal{J} = 0. \qquad (13)$$

Then, the three roots of the above cubic equation κ_1, κ_2 and κ_3 should satisfy the following transcendental equation

$$\begin{aligned}\mathcal{R}e^{-\alpha L}e^{-i(2k_0L - i\frac{\nu}{d_1})}[(\kappa_1^2 - Q)(\kappa_2 - \kappa_3)\\ +(\kappa_2^2 - Q)(\kappa_3 - \kappa_1) + (\kappa_3^2 - Q)(\kappa_1 - \kappa_2)]\\ +(\kappa_1^2 - Q)(\kappa_2 - \kappa_3)e^{\kappa_1} + (\kappa_2^2 - Q)(\kappa_3 - \kappa_1)e^{\kappa_2}\\ +(\kappa_3^2 - Q)(\kappa_1 - \kappa_2)e^{\kappa_3} = 0. \qquad (14)\end{aligned}$$

By solving the above two equations, we can find out the minimum value of $\mathcal{J}$, called the dimensionless start current $\mathcal{J}_s$ for a given Q, $\mathcal{R}$, α and L, for which the real part of the complex growth rate ν is positive.

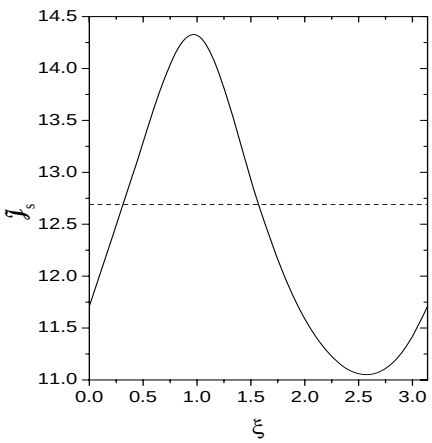

Figure 1: Variation in the dimensionless start current with ξ for $\mathcal{R}$ = 0.8 (solid curve) and $\mathcal{R}$ = 0 (dashed curve).

Next, we use Eqs. (13-14) for the calculation of start current. In a companion paper [4], we have optimized the parameters corresponding to Dartmouth experiment [6] taking attenuation into account, but excluding end reflection. We use those parameters for calculation of start current here. For the grating, we use groove depth d = 150 μm, groove width w = 110 μm, period λ_g = 173 μm and length L = 12.7 mm. For the 35 keV sheet electron beam, we use b = 10 μm. From our calculation [2], for these parameters, we obtain the free-space wavelength λ = 819 μm, χ = 120 per cm, χ_1 = 3.9, $\alpha L = 0.94(1 - i)$ and v_g/c = 0.0925. Note that in Eq. (14), for a given grating length, when we change the electron beam energy, the value of k_0 will change, which will change the phase factor term e^{-2ik_0L}. Let us define ξ = mod(k_0L, π). Hence, for a given set of parameters, if we make a slight change in the electron beam energy, the value of ξ changes accordingly and affects the value of start current. For our parameters, Q is very small, and we take Q = 0. Figure 1 shows the variation of dimensionless start current $\mathcal{J}_s$ with ξ for $\mathcal{R}$ = 0.8. We find that that the value of $\mathcal{J}_s$ oscillates between 11.1 and 14.2. Note that the start current density corresponding to $\mathcal{J}$ = 11.1 is 4.7 mA/mm. The value of $\mathcal{J}_s$ is 12.7, when we neglect end reflection. When the attenuation is smaller, the effect of end reflection is more pronounced.

NUMERICAL SIMULATION

For numerically solving Eqs. (4-7), we use the approach used by Ginzburg et al. [7] and later also by Levush et al. [8] for BWO. The electron dynamics equations for a given field distribution along the interaction region are solved by the predictor-corrector method. Then, knowing the modified electron distribution in phase space, the field distribution at the next time step is obtained by solving the partial differential equations (Eqs. 4-5) by the finite difference method. The method is stable for $\Delta\tau < \Delta\zeta$ for the backward wave and for $\Delta\tau < (1/d_1)\Delta\zeta$ for the forward wave. Here, $\Delta\tau$ and $\Delta\zeta$ are the step sizes in τ and ζ respectively, used in the finite difference method.

For initializing the electron beam in phase space, we simulate the shot noise using the algorithm given by Penman and McNeil [9], which is commonly used in FEL codes.

We performed a couple of tests on the code we developed. We first checked for the convergence of the solution by increasing the number of particles and also by reducing the step size. Based on this convergence test, we chose the number of particles to be used in the simulation as 1024 and the step sizes as $\Delta\tau$ = 0.01 and $\Delta\zeta$ = 0.02. We also confirmed that the energy conservation equation along with the damping term due to attenuation is satisfied in the code at each integration step.

Figure 2 shows the evolution of power in the backward wave at the entrance of the grating for $\mathcal{J}$ = 11.6 and $\mathcal{J}$ = 10.6. The parameters used in the calculation are same as mentioned in the last section. We have chosen ξ = 2.5 for which $\mathcal{J}_s$ is minimum as shown in Fig. 1. For these parameters, $\mathcal{J}_s$ = 11.1 and hence for the case $\mathcal{J}$ = 10.6, there is no build-up of power, whereas for the case $\mathcal{J}$ = 11.6, we find that the power grows exponentially and saturates. Note that $I/\Delta y$ = 4.9 mA/mm for $\mathcal{J}$ = 11.6. After saturation, the variation of the amplitude of electric field for the forward as well as the backward wave along the length of the grating is shown in Fig. 3.

Let us now discuss the calculation of outcoupled power. Power in the backward and the forward surface mode denoted by P_- and P_+ respectively can be obtained by the following expression

$$\frac{P}{\Delta y} = 2\frac{\beta\gamma}{Z_0\chi}\left(\frac{mc^2\beta^3\gamma^3}{ek_0L^2}\right)^2 e^{2\Gamma_0 b}|\mathcal{E}|^2, \qquad (15)$$

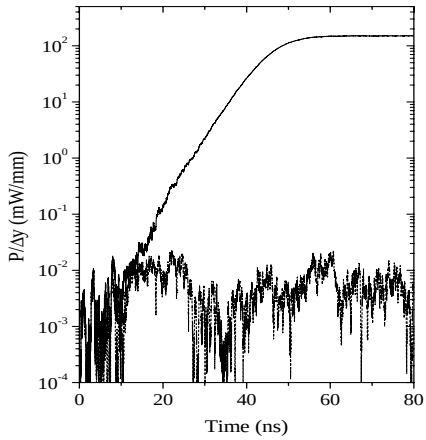

Figure 2: Evolution of power in the backward wave at the entrance of the undulator for $\mathcal{J}$ = 11.6 (solid curve), and $\mathcal{J}$ = 10.6 (dashed curve). We have used $\mathcal{R}$ = 0.8 and ξ = 2.5 in the calculation.

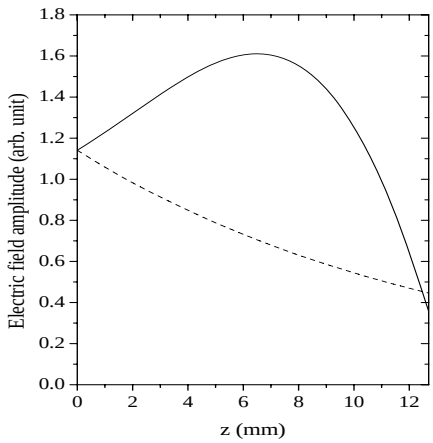

Figure 3: Variation of the amplitide $|\mathcal{E}_-|$ of the backward wave (solid curve) and the amplitude $|\mathcal{E}_+|$ of the forward wave (dashed curve) along the length of the grating for $\mathcal{J}$ = 11.6. Other parameters are same as those used in Fig. 2.

where $P = P_-$ for $\mathcal{E} = \mathcal{E}_-$ and $P = P_+$ for $\mathcal{E} = \rho_0\mathcal{E}_+$. The outcoupled power P_0 at the entrance of the grating is given by $P_-(z = 0) - P_+(z = 0)$ and at the exit, the outcoupled power P_1 is given by $P_+(z = L) - P_-(z = L)$. If we assume $\rho_L = 1$, the power will be outcoupled only at the entrance of the grating. For the case of Fig. 3, the outcoupled power is calculated to be 54 mW for Δy = 1 mm. The total power in the electron beam for this case is 171.5 W for 35 keV, 4.9 mA electron beam current. Hence, the overall efficiency is only 0.03%. Such a low efficiency is there beacuse we have chosen the electron beam current very close to the start current and also the heat loss occurring in the grating due to attenuation deteriorates the efficiency. We have checked that the efficiency is improved at higher value of beam current. Our emphasis here is to show that including reflection, it is possible to reduce the start current surface density to as low as 4.7 mA/mm.

In our calculation, we have not calculated the value of reflectivity, instead we have assumed a value for reflectivity. In a realistic situation, there will be some reflectivity at the end of the grating due to change of boundary, which needs to be calculated. However, we can put an external mirror and the reflectivity $\mathcal{R}$ can be adjusted to a desired value. By introducing a reflectivity, the start current is reduced, but the outcoupled power may not be optimized. Using our calculation in the saturation regime, one can optimize the parameters to obtain optimum combination of start current and outcoupled power.

CONCLUSIONS

In this paper, we have set up Maxwell-Lorentz equations for the one-dimensional time-dependent analysis of SP-BWO including end reflection and attenuation due to finite conductivity. We have obtained a solution in the linear regime and extended the analysis to the nonlinear regime by solving the Maxwell-Lorentz equations numerically. Our analysis can be used for detailed optimization of outcoupled power and start current in SP-BWO taking end reflection and attenuation into account.

REFERENCES

[1] H. L. Andrews and C. A. Brau, Phys. Rev. ST Accel. Beams, 7 (2004) 070701.

[2] V. Kumar and K.-J. Kim, Phys. Rev. E 73 (2006) 026501.

[3] H. L. Andrews et al., Phys. Rev. ST Accel. Beams, 8 (2005) 050703.

[4] V. Kumar and K.-J. Kim, these proceedings

[5] R. Bonifacio, C. Pelligrini, and L. M. Narducci, Opt. Commun. **40** 373 (1984).

[6] J. Urata et al., Phys. Rev. Lett. 80 (1998) 516.

[7] N. S. Gingburg, S. P. Kuznetov, and T. N. Fedoseeva, Sov. Radiophys. Electron., 21 (1979) 728.

[8] B. Levush et al., IEEE Trans. Plasma Sci. 20, (1992) 263.

[9] C. Penman and B. W. J. McNeil, Opt. Commun. 90 (1992) 82.